

DISCOVERY OF A CANDIDATE PROTOPLANETARY DISK AROUND THE EMBEDDED SOURCE IRC9 IN ORION¹

Nathan Smith² and John Bally

*Center for Astrophysics and Space Astronomy, University of Colorado, 389 UCB, Boulder, CO 80309;
nathans@casa.colorado.edu*

ABSTRACT

We report the detection of spatially-extended mid-infrared emission around the luminous embedded star IRC9 in OMC-1, as seen in 8.8, 11.7, and 18.3 μm images obtained with T-ReCS on Gemini South. The extended emission is asymmetric, and the morphology is reminiscent of warm dust disks around other young stars. The putative disk has a radius of roughly $1''.5$ (700 AU), and a likely dust mass of almost 10 Earth masses. The infrared spectral energy distribution of IRC9 indicates a total luminosity of $\sim 100 L_{\odot}$, implying that it shall become an early A-type star when it reaches the main sequence. Thus, the candidate disk around IRC9 may be a young analog of the planetary debris disks around Vega-like stars and the disks of Herbig Ae stars, and may provide a laboratory in which to study the earliest phases of planet formation. A disk around IRC9 may also add weight to the hypothesis that an enhanced T Tauri-like wind from this star has influenced the molecular outflow from the OMC-1 core.

Subject headings: planetary systems: protoplanetary disks — stars: formation — stars: pre-main-sequence

1. INTRODUCTION

One of the most spectacular bipolar protostellar outflows known is the system of H₂ “fingers” emanating from the BN/KL region in the OMC-1 cloud core (Allen & Burton 1993; Schild et al. 1997; Kaifu et al. 2000), at a distance of roughly 460 pc (Bally et al. 2000). Among the embedded infrared (IR) sources associated with the BN/KL complex, the bright source IRC9 (Downes et al. 1981; Wynn-Williams & Becklin 1974) is relatively isolated, located $\sim 30''$ north of the rest of BN/KL (see Fig. 1a). The H₂ outflow from BN/KL appears highly asymmetric, with the northwest/blueshifted part of the flow being brighter and more extended. This asymmetry is not easily explained by the tilt angle and corresponding potential extinction of the redshifted flow, since observations of H₂ at both 2.12 μm and 12.3 μm show the same degree of asymmetry (Beck 1984). Suspiciously, IRC9 is found near the H₂ emission peak within the brighter northwest part of the bipolar outflow. This may be a simple coincidence, but Beck (1984) has proposed the alternative view that IRC9 may have had a direct role in influencing the asymmetric appearance the BN/KL outflow. Specifically, Beck (1984) suggests that a T Tauri-like wind from IRC9, if it exists, may have helped create a lower density

¹Based on observations obtained at the Gemini Observatory, which is operated by the Association of Universities for Research in Astronomy, Inc., under a cooperative agreement with the NSF on behalf of the Gemini partnership: the National Science Foundation (US), the Particle Physics and Astronomy Research Council (UK), the National Research Council (Canada), CONICYT (Chile), the Australian Research Council (Australia), CNPq (Brazil), and CONICET (Argentina).

²Hubble Fellow

region, allowing the northwest part of the BN/KL outflow to escape to larger distances with higher speeds than the southeast counterflow. A direct link between IRc9 and the H₂ outflow is supported by unusual kinematics seen in spectra of the 12.28 μm H₂ emission line, which reveal that the most complex line shapes are found in the region near IRc9 (Beck et al. 1982). Thus, while IRc9 does not give rise to the H₂ outflow itself, it is a good candidate for influencing the outflow’s asymmetry.

In this Letter we report the detection of a spatially-extended asymmetric dust envelope around IRc9, probably representing a large circumstellar disk. The presence of a disk would add weight to the hypothesis that IRc9 is a young star with an active outflowing wind analogous to T Tauri stars, as required in the scenario proposed by Beck (1984). However, even if Beck’s interpretation is incorrect, the extended emission we report here suggests that IRc9 is an interesting source in its own right because it may be surrounded by a very young protoplanetary disk. The integrated luminosity of IRc9 suggests that when it eventually reaches the main-sequence, it will be an early A-type star. Therefore, the disk around IRc9 may also provide an example of the youngest phases in a planet-forming disk that will eventually evolve into a debris disk analogous to those seen around Vega-like stars.

2. OBSERVATIONS

On 2004 Jan 25, 26, and 27 we used T-ReCS¹ on Gemini South to obtain 8.8, 11.7, and 18.3 μm images of IRc9, located about 30'' north of the BN/KL nebula in Orion (see Fig. 1*a*). T-ReCS is Gemini South’s facility mid-IR imager and spectrograph with a 320×240 pixel Si:As IBC array, a pixel scale on the 8m telescope of 0''.089, and a resulting field-of-view of 28''.5×21''.4. The observations were taken with a 15'' east-west chop throw, and a chopping frequency of a few Hz (different for each filter). In each filter, 4 spatially-offset groups of chop-nod pairs (each composed of 10 individual pairs) were combined to make the final image, using the central peak of IRc9 itself for spatial alignment. These observations were part of a larger wide-field mosaic of Orion, and additional T-ReCS images of Orion from this same dataset were presented in an earlier paper (Smith et al. 2004).

Figures 1*b*, *c*, and *d* show the resulting 8.8, 11.7, and 18.3 μm images of IRc9. The images were flux calibrated using observations of the secondary standard star HD 32887, adopting the values tabulated by Cohen et al. (1999). Absolute photometric uncertainty is probably dominated by the ~5% uncertainty in the calibration, rather than the 1σ noise-equivalent flux density in the background for an aperture of the same size given in Table 1. The nights were photometric during the 8.8 and 11.7 μm observations, and the sky was photometric for the early part of the 18.3 μm mosaic when IRc9 was observed, although conditions deteriorated later in the night. Background-subtracted photometry for IRc9 is listed in Table 1, measured in a 5''.3 diameter aperture to include all the extended structure visible in images.

To clarify the extended structure around IRc9, we subtracted a scaled point spread function (PSF) from the images (Figs. 1*e*, *f*, and *g*), and Table 1 also lists the corresponding flux of the star that was subtracted and the residual emission left after the PSF subtraction. The PSF used for subtraction in each filter was the corresponding observation of the standard star, obtained ~10 min before the 8.8 and 18.3 μm observations, and ~25 min prior to the 11.7 μm observation of IRc9. The empirical PSF was scaled and subtracted from each of the IRc9 images in a somewhat subjective manner – chosen to minimize residual emission near the star without severely over-subtracting the central PSF (i.e. to avoid creating negative

¹<http://www.gemini.edu/sciops/instruments/miri/MiriIndex.html>.

flux values). Uncertainty in the residual flux may be as high as 30% at 8.8 μm where the central star was bright compared to the total extended flux, but the photometric uncertainty in the residual flux at 18.3 μm is comparable to the $\sim 5\%$ calibration uncertainty because the extended emission constitutes the majority of the flux from IRc9 at that wavelength. Obviously the uncertainty in the residual structure is highest near the position of the star where small differences in the PSF may leave the most severe artifacts (especially at the shorter wavelengths). However, structure beyond 1'' from the star's position is much more reliable, and the uncertainty there is comparable to the statistical uncertainty (the lowest contour is drawn at 3σ above the background in Figs. 1 *efg*).

3. RESULTS

Figure 1 shows that IRc9 is an extended object, with a size of 3–4'', elongated roughly along P.A. $\simeq 120^\circ$. This elongated structure is evident both before and after subtraction of the central point source. Given the shape of the extended emission, it is likely that the central star powering IRc9 is surrounded by a large dusty circumstellar disk, with the polar axis oriented at P.A. $\simeq 30^\circ$. The residual emission after the PSF subtraction is spatially-resolved along both the minor and major axes of the nebula; if this is a tilted circular disk then the difference between the major and minor dimensions suggests that its polar axis is inclined from the plane of the sky by perhaps 30° .

Is this emission really from a disk? An alternative view might be that this represents externally-illuminated material in the OMC-1 cloud core, as is the case for many of the complex dust structures seen in the BN/KL nebula (e.g., Shuping et al. 2004). While this interpretation is difficult to refute conclusively with the present dataset, we consider it less likely than the disk hypothesis because IRc9 is relatively isolated from the BN/KL core (see Fig. 1a), and no other point source out of 83 that we detected in our larger mosaic of the inner Orion nebula shows similar extended structure. The diameter of this putative disk (1400–1800 AU) is comparable to or somewhat larger than the largest proplyd silhouette disks in Orion (Bally et al. 2000; Shuping et al. 2003; Smith et al. 2004a), and is similar to the sizes of several disk candidates seen in the Carina nebula (Smith et al. 2003).

IRc9's disk is brighter on the southeast side, with the brightness asymmetry being most pronounced (roughly a factor of 2) at the longest wavelength. Interestingly, the bright part of the disk faces toward the heart of the BN/KL complex. If this apparent asymmetry arises because a portion of IRc9's disk is heated externally by the BN/KL central engine or by interaction with its molecular outflow, this would provide evidence that the two objects are indeed at the same distance.

The spectral energy distribution (SED) of IRc9 is shown in Figure 2, including the total flux, the subtracted PSF, and the residual emission from Table 1. This SED obviously cannot be reproduced with a single-temperature dust model, so Figure 2 shows a simple fit using three individual temperature components at 750, 170, and 115 K. These individual components are guided by the spatially-resolved photometry in Table 1, plotted in Figure 2. The 750 and 170 K components together constitute the central PSF source that was subtracted, while the cooler 115 K dust component matches the flux from the residual emission after the PSF was subtracted (Figs. 1*e*, *f*, and *g*). The central point-like source is probably a mix of reddened photospheric emission and a range of hot dust temperatures in a compact ($R < 160$ AU) disk around the star. The 115 K component represents optically-thin emission from cooler dust in the extended circumstellar disk. The integrated luminosity of each component and the total of all three are listed in Table 2. If the dust grains are small ($a < 0.2 \mu\text{m}$) the dust mass required to emit this IR luminosity can be expressed independent

of the grain radius and emissivity (see Smith & Gehrz 2005), so that $M_{\text{dust}} = [(100\rho)/(3\sigma T^6)] L_{\text{IR}}$. This relation was used to derive the dust masses for each component in Table 2. If the dominant dust grains are large ($a > 1 \mu\text{m}$) then the mass estimate is more uncertain and far-IR or submillimeter measurements are probably needed. (However, we do not see an obvious reason why large grains would dominate the grain size distribution in the outer disk for this embedded source, which is shielded from the strong external UV radiation field of the Trapezium.)

Most of the mass resides in the coolest extended component (about $8 M_{\oplus}$), indicating that the disk around IRc9 provides a significant reservoir out of which planets may potentially form. Note, however, that since we ignored extinction and since optically-thick regions may be present in the inner disk, the mass estimates for the 750 and 170 K components are really a lower limit to the mass of the warm inner parts of the disk. The dust temperature of 115 K in the extended disk is consistent with the equilibrium temperature for small ($a \simeq 0.1 \mu\text{m}$) grains at a separation of $1''$ (460 AU) from a central source with a luminosity of ~ 100 – $200 L_{\odot}$ (assuming $Q_{\text{abs}}/Q_{\text{em}} \approx 100$ for small grains; see Smith & Gehrz 2005 and references therein). This is roughly consistent with or somewhat higher than the integrated IR luminosity of IRc9 (Table 2), perhaps suggesting that some of the source luminosity may escape in directions not intercepted by the disk.

4. DISCUSSION

If the extended mid-IR emission around IRc9 really does represent a circumstellar disk, then it has two important ramifications. An active accretion disk around IRc9 would suggest that it is a very young pre-main-sequence star. This would add plausibility to the hypothesis that it has a strong T Tauri-like mass-loss wind that could have potentially affected the appearance of the bipolar molecular outflow from BN/KL (Beck 1984), although this hypothesis remains speculative. Additional evidence that IRc9 may be a very young object comes from its Br γ emission (Beck 1984). If IRc9 is embedded in the outflow from the BN/KL region, could it survive? Embedded in the OMC-1 cloud, IRc9 is shielded from photoablation by the intense UV radiation of the Trapezium, where protoplanetary disks are thought to survive for 10^5 yr or more (O’Dell 1998), whereas the dynamical time of the BN/KL outflow is only about 1000 yr (Lee & Burton 2000; Doi et al. 2002). Estimating the disk’s ability to survive dynamical interaction with shocks caused by the BN/KL outflow itself is more difficult, and probably requires a numerical investigation beyond the scope of this Letter.

Even more tantalizing is that a young disk around IRc9 may provide a laboratory to study the earliest phases of planet formation. Recent studies of several A-type stars have revealed extended thermal-IR emission from dust in planetary debris disks. Some well-known examples are the disks around β Pic (A5 V; Wahhaj et al. 2003; Weinberger et al. 2003), HR 4796A (A0 V; Koerner et al. 1998; Jayawardhana et al. 1998; Schneider et al. 1999), Fomalhaut (A3 V; Holland et al. 2003), HD 141569 (B9.5 Ve; Weinberger et al. 1999), and Vega itself (Holland et al. 1998). These Vega-like stars are typically a few to tens of Myr old – older than expected timescales for planet formation – so mature planets have presumably already formed, and their disks are probably the remnants of the planet formation process. The dust in these disks is thought to be replenished from collisions of planetesimals (Backman & Paresce 1993). These debris disks typically have radii somewhat smaller than that of IRc9, but significantly lower masses. It is intriguing that the apparent size, mass, and the mildly asymmetric structure of the material around IRc9 are reminiscent of the disk and envelope around the Herbig Ae star AB Aurigae (Fukugawa et al. 2004).

The integrated luminosity of IRc9 is roughly $100 L_{\odot}$, which places it on a pre-main-sequence track for

a star that will eventually have $M_{\text{ZAMS}} \simeq 3\text{--}4 M_{\odot}$ and an early A spectral type (e.g., Marconi & Palla 2004). Thus, the disk around IRC9 may be an early analog of these more evolved debris disks, and so we speculate that it is a good candidate for a very young protoplanetary disk around a Vega-like star. If true, IRC9 may be a valuable laboratory for studying the earliest phases of planet formation. In any case, IRC9 certainly deserves closer scrutiny.

Support for N.S. was provided by NASA through grant HF-01166.01A from the Space Telescope Science Institute, which is operated by the Association of Universities for Research in Astronomy, Inc., under NASA contract NAS5-26555. We thank an anonymous referee for several suggestions that improved the presentation of our results.

REFERENCES

- Allen, D.A., & Burton, M.G. 1993, *Nature*, 353, 54
- Backman, D.E., & Paresce, F. 1993, in *Protostars and Planets III*, ed. E.H. Levy & J.I. Lunine (Tucson: U. Arizona Press), 1253
- Bally, J., O'Dell, C.R., & McCaughrean, M.J. 2000, *AJ*, 119, 2919
- Beck, S.C. 1984, *ApJ*, 281, 205
- Beck, S.C., Bloemhof, E.E., Serabyn, E., Townes, C.H., Tokunaga, A.T., Lacy, J.H., & Smith, H.A. 1982, *ApJ*, 253, L83
- Cohen, M., Walker, R.G., Carter, B., Hammersley, R., Kidger, M., & Nogushi, K. 1999, *AJ*, 117, 1864
- Doi, T., O'Dell, C.R., & Hartigan, P. 2002, *AJ*, 124, 445
- Downes, D., Genzel, R., Becklin, E.E., & Wynn-Williams, C.G. 1981, *ApJ*, 244, 869
- Fukugawa, H., et al. 2004, *ApJ*, 605, L53
- Holland, W.S., et al. 1998, *Nature*, 392, 788
- Holland, W.S., et al. 2003, *ApJ*, 582, 1141
- Jayawardhana, R., Fisher, S., Hartmann, L., Telesco, C., Pina, R., & Fazio, G. 1998, *ApJ*, 503, L79
- Kaifu, N., et al. 2000, *PASJ*, 52, 1
- Koerner, D.W., Ressler, M.E., Werner, M.W., & Backman, D.E. 1998, *ApJ*, 503, L83
- Lee, J.K., & Burton, M.G. 2000, *MNRAS*, 315, 11
- Marconi, M., & Palla, F. 2004, *IAU Symp.* 224, 119
- O'Dell, C.R. 1998, *AJ*, 115, 263
- Schild, H., Miller, S., & Tennyson, J. 1997, *A&A*, 318, 608
- Schneider, G., et al. 1999, *ApJ*, 513, L127
- Shuping, R.Y., Morris, M., & Bally, J. 2004, *AJ*, 128, 363
- Shuping, R.Y., Bally, J., Morris, M., & Throop, H. 2003, *ApJ*, 587, L109
- Smith, N., Bally, J., & Morse, J.A. 2003, *ApJ*, 587, L105
- Smith, N., Bally, J., Licht, D., & Walawender, J. 2004a, *AJ*, 129, 382
- Smith, N., Bally, J., Shuping, R.Y., Morris, M., & Hayward, T.L. 2004b, *ApJ*, 610, L117
- Smith, N., & Gehrz, R.D. 2005, *AJ*, 129, 969
- Wahhaj, Z., Koerner, D.W., Ressler, M.E., Werner, M.W., Backman, D.E., & Sargent, A.I. 2003, *ApJ*, 584, L27
- Weinberger, A.J., Becklin, E.E., & Zuckerman, B. 2003, *ApJ*, 584, L33
- Weinberger, A.J., et al. 1999, *ApJ*, 525, L53
- Wynn-Williams, C.G., & Becklin, E.E. 1974, *PASP*, 86, 5

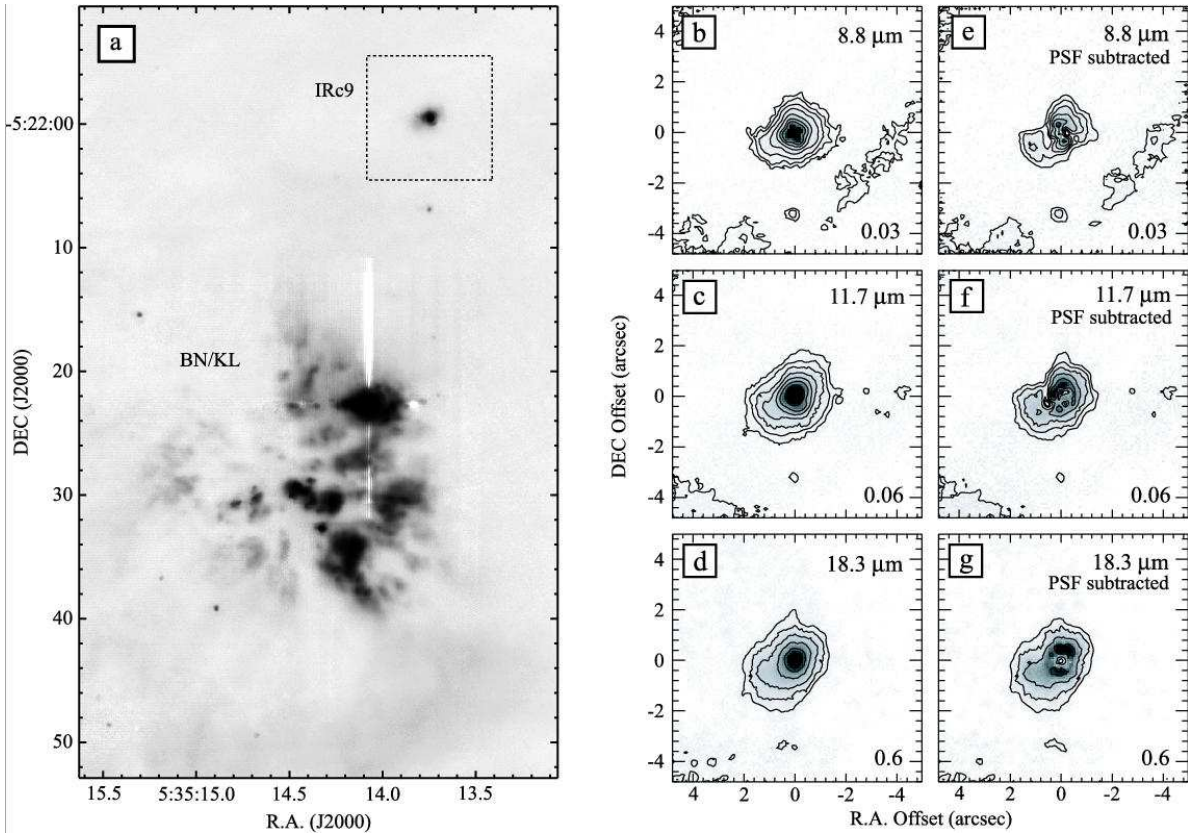


Fig. 1.— (a) Northern portion of our $11.7 \mu\text{m}$ image mosaic of the Orion nebula. (b, c, d) Raw images of IRC9 at 8.8 , 11.7 , and $18.3 \mu\text{m}$, respectively, corresponding to the box in Panel a. (e, f, g) Same as neighboring images, except that an observed PSF has been subtracted. In Panels b–g, the lowest contour level in Jy arcsec^{-2} is given in the lower right corner, and each subsequent contour level is a factor of 2 above the previous one.

Table 1. Observations and Photometry of IRC9

| Parameter | Units | 8.8 μm | 11.7 μm | 18.3 μm |
|------------------------|---------------|-------------------|--------------------|--------------------|
| filter $\Delta\lambda$ | μm | 0.78 | 1.13 | 1.5 |
| exp. time | sec. | 72 | 72 | 72 |
| 1σ F_ν | mJy | 8.3 | 10.5 | 66 |
| F_ν total | Jy | 5.85 | 9.46 | 30.5 |
| F_ν star | Jy | 5.25 | 6.85 | 10.9 |
| F_ν PSFsub | Jy | 0.60 | 2.61 | 19.6 |
| FWZI ^a | arcsec | 3.0 | 3.6 | 4.0 |

^aSize of the major-axis diameter of the PSF-subtracted emission at the lowest contour level.

Table 2. Luminosity and Dust Mass

| Component | L_{IR} (L_\odot) | M_{dust} (M_\oplus) |
|-----------|----------------------------------|-------------------------------------|
| 750 K | 40 | 8.8×10^{-5} |
| 170 K | 14 | 0.22 |
| 115 K | 48 | 8.1 |
| Total | 102 | 8.3 |

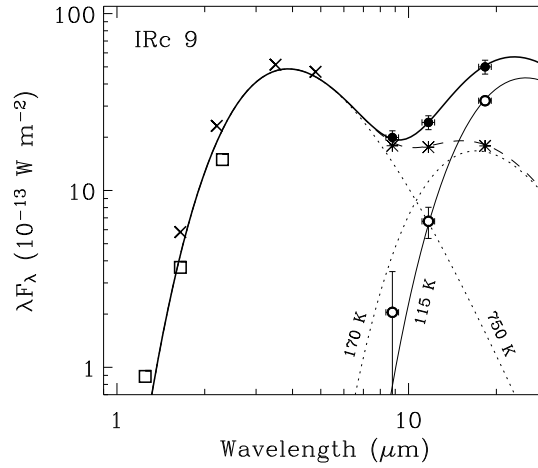


Fig. 2.— The spectral energy distribution of IRC9. Filled circles are the total flux in a $5''.3$ diameter aperture measured in T-ReCS images, unfilled circles are the PSF-subtracted flux, and stars represent the PSF flux that was subtracted. Unfilled squares are 2MASS data, and X's are photometric measurements by Wynn-Williams & Becklin (1974). The various curves are individual Planck functions fit to the data with a λ^{-1} emissivity, or the sum of those Planck functions. The thin solid line represents the extended 115 K emission, the dashed line is the central point-like source (the sum of the dotted curves for the 750 and 170 K components), and the heavy solid line is the total emission.